

000 BEYOND MEMBERSHIP: LIMITATIONS OF 001 ADD/REMOVE ADJACENCY IN DIFFERENTIAL 002 PRIVACY 003

006 **Anonymous authors**

007 Paper under double-blind review

010 ABSTRACT

013 Training machine learning models with differential privacy (DP) limits an adver-
014 sary’s ability to infer sensitive information about the training data. It can be in-
015 terpreted as a bound on adversary’s capability to distinguish two adjacent datasets
016 according to chosen adjacency relation. In practice, most DP implementations use
017 the add/remove adjacency relation, where two datasets are adjacent if one can be
018 obtained from the other by adding or removing a single record, thereby protecting
019 membership. In many ML applications, however, the goal is to protect attributes
020 of individual records (e.g., labels used in supervised fine-tuning). We show that
021 privacy accounting under add/remove overstates attribute privacy compared to ac-
022 counting under the substitute adjacency relation, which permits substituting one
023 record. To demonstrate this gap, we develop novel attacks to audit DP under
024 substitute adjacency, and show empirically that audit results are inconsistent with
025 DP guarantees reported under add/remove, yet remain consistent with the budget
026 accounted under the substitute adjacency relation. Our results highlight that the
027 choice of adjacency when reporting DP guarantees is critical when the protection
028 target is per-record attributes rather than membership.

029 1 INTRODUCTION

031 Differential Privacy (DP) (Dwork et al., 2006) provides provable protection against the most com-
032 mon privacy attacks, including membership inference, attribute inference and data reconstruction
033 (Salem et al., 2023). It limits an adversary’s ability to distinguish between two adjacent datasets
034 based on the an algorithm’s output. The level of DP guarantee depends on the underlying adjacency
035 relation. There exist different notions of adjacency such as the *add/remove* adjacency, where two
036 datasets differ by the inclusion or removal of a single record. An alternative is *substitute* adjacency,
037 where one dataset is obtained by replacing a record in the other. A special case of the latter is
038 *zero-out* adjacency, in which a record is replaced with a null entry. In deep learning (Abadi et al.,
039 2016; Ponomareva et al., 2023), the standard approach to DP uses add/remove adjacency, that was
040 designed to protect against an adversary’s ability to detect whether an individual was part of the
041 training dataset or not.

042 In this paper, we draw attention to the fact that while DP can provide protection against all the
043 common attacks listed above, the add/remove adjacency does not provide protection against inference
044 attacks on data of a subject known to be a part of the training dataset at the level indicated
045 by the privacy parameters. Protection against such inference attacks requires considering substitute
046 adjacency, which protects against inference of a single individual’s contribution to the data. An
047 add/remove privacy bound implies a substitute privacy bound, but with substantially weaker privacy
048 parameters. Most DP libraries (such as Opacus Yousefpour et al. (2021)) implement privacy ac-
049 counting assuming add/remove adjacency. A practitioner concerned with attribute or label privacy
050 who relies on these libraries to train their model with DP may therefore be misled: the guarantees
051 provided by add/remove adjacency overstate the actual protection against attribute inference attacks.

052 In order to evaluate practical vulnerability of DP models and mechanisms to substitute-type attacks,
053 we develop a range of auditing tools for the substitute adjacency and apply these to DP deep learning.
In this setting, we craft a pair of neighbouring datasets, \mathcal{D} and \mathcal{D}' by replacing a target record $z \in \mathcal{D}$

054 with a canary record z' . A canary serves as a probe that enables the adversary to determine whether
 055 a model was trained on \mathcal{D} or \mathcal{D}' . We find that the algorithms do indeed leak more information to a
 056 training data inference attacker than the add/remove bound would suggest.
 057

058 **Our Contributions:**
 059

060 • We propose algorithms for crafting canaries for auditing DP under substitute adjacency, provid-
 061 ing tight empirical lower bounds matching theoretical guarantees from accountants (Section 3).
 062 • We show that privacy leakage can exceed the guarantees derived from add/remove accountants
 063 but (as expected), closely tracks the guarantees predicted by substitute accountants (Section 6).
 064 • Our results demonstrate that accounting for privacy under the commonly used add/remove ad-
 065 jacency overstates the protection against attribute inference, including label inference.
 066

067 **2 RELATED WORK AND PRELIMINARIES**
 068

069 **2.1 DIFFERENTIAL PRIVACY**
 070

071 Differential Privacy (DP) (Dwork et al., 2006) is a framework to protect sensitive data used for data
 072 analysis with provable privacy guarantees.

073 **Definition 1** $((\varepsilon, \delta, \sim)$ -Differential Privacy). *A randomized algorithm \mathcal{M} is $(\varepsilon, \delta, \sim)$ -differentially
 074 private if for all pairs of adjacent datasets $\mathcal{D} \sim \mathcal{D}'$, and for all events S :*
 075

$$076 \Pr[\mathcal{M}(\mathcal{D}) \in S] \leq e^\varepsilon \Pr[\mathcal{M}(\mathcal{D}') \in S] + \delta, \\ 077$$

078 Under add/remove adjacency (\sim_{AR}), \mathcal{D}' is obtained by adding or removing a record z from \mathcal{D} . In
 079 substitute adjacency (\sim_S), \mathcal{D}' is formed by replacing a record z in \mathcal{D} with another record z' . Kairouz
 080 et al. (2021) also introduced the zero-out adjacency which corresponds to removing a record from
 081 \mathcal{D} and replacing it with a zero-out record (\perp) to form \mathcal{D}' . Privacy guarantees for this adjacency are
 082 semantically equivalent to the add/remove DP.
 083

084 **2.2 DIFFERENTIALLY PRIVATE STOCHASTIC GRADIENT DESCENT (DP-SGD)**
 085

086 Differentially Private Stochastic Gradient Descent (DP-SGD) (Rajkumar & Agarwal, 2012; Song
 087 et al., 2013; Abadi et al., 2016) forms the basis of training machine learning algorithms with DP. It
 088 is used to train ML models while satisfying DP. Given a minibatch $B_t \in \mathcal{D}$ at time step t , DP-SGD
 089 first clips the gradients for each sample in B_t such that the ℓ_2 norm for per-sample gradients does not
 090 exceed the clipping bound C . Following that, Gaussian noise with scale σC is added to the clipped
 091 gradients. These clipped and noisy gradients are then used to update the model parameters θ during
 092 training as follows:
 093

$$094 \theta_{t+1} \leftarrow \theta_t - \frac{\eta}{|B|} \left[\sum_{z \in B_t} \text{clip}(\nabla_\theta \ell(\theta_t; z), C) + Z_t \right], \quad (1) \\ 095$$

096 where $Z_t \sim \mathcal{N}(0, \sigma^2 C^2 \mathbb{I})$, $|B|$ is the expected batch size, and η denotes the learning rate of the
 097 training algorithm. In this way, DP-SGD bounds the contribution of an individual sample to train
 098 the model. In this paper, we also use DP-Adam which is the differentially private version of the
 099 Adam (Kingma & Ba, 2015) optimizer.
 100

101 DP provides upper bounds for the privacy loss expected from an algorithm for a given adjacency re-
 102 lation. Early works used advanced composition (Dwork et al., 2010; Kairouz et al., 2015) to account
 103 for the cumulative privacy loss over multiple runs of a DP algorithm. Abadi et al. (2016); Mironov
 104 (2017); Bun & Steinke (2016) developed accounting methods for deep learning algorithms. How-
 105 ever, the bounds on DP parameters provided by these accountants are not always tight. Recently,
 106 numerical accountants based on privacy loss random variables (PRVs) (Dwork & Rothblum, 2016;
 107 Meiser & Mohammadi, 2018) have been adopted across industry and academia (Koskela et al., 2020;
 108 Gopi et al., 2021) because they offer tighter estimates of DP upper bounds.
 109

108 2.3 AUDITING DIFFERENTIAL PRIVACY
109

110 Privacy auditing helps evaluate the empirical privacy leakage from a differentially private machine
111 learning algorithm. DP auditing involves assessing the privacy it affords to worst-case canary
112 records. Jayaraman & Evans (2019) were the first to evaluate the empirical privacy leakage from
113 machine learning models trained with DP-SGD and revealed a large gap between the empirical leakage
114 and the theoretical bounds guaranteed by DP-SGD. Later, Nasr et al. (2021) audited DP machine
115 learning algorithms under progressively stronger threat models. They show that the empirical pri-
116 vacy leakage from their strongest threat model using worst-case dataset canaries was “tight” with
117 respect to the privacy accounting upper bound for DP. Subsequent works such as Nasr et al. (2023);
118 Steinke et al. (2023); Annamalai & Cristofaro (2024); Zanella-Béguin et al. (2023); Mahloujifar
119 et al. (2025); Cebere et al. (2025) have since been focused on crafting worst-case canary records
120 that could yield tight auditing for models trained with natural datasets with the more recent works
121 focusing on practical threat models.

122 Threat models in auditing differ by the adversary’s level of access: in the *White-Box* setting, the
123 adversary can access the intermediate models during training (Nasr et al., 2021; 2023; Steinke et al.,
124 2023); in the more realistic *Hidden-State* setting, the adversary can only access the final model but
125 may still perturb inputs to intermediate models (Annamalai, 2024; Cebere et al., 2025); and in the
126 *Black-Box* setting (Annamalai & Cristofaro, 2024; Boglioni et al., 2025), the adversary can only
127 insert canary sample(s) at the start of training and tracks the final trained model’s response on these
128 canary sample(s).

129 3 AUDITING DP WITH SUBSTITUTE ADJACENCY
130

131 Our goal is to design canary samples for auditing DP under substitute adjacency in a *hidden-state*
132 threat model. In this setting, the adversary can only access the final model at any step t , without visibility
133 into prior intermediate models. Table 1 briefly describes the crafting scenarios for canaries used to
134 audit DP with substitute adjacency. In Table 2, we detail the adversary’s prior knowledge in each scenario.
135 Algorithm 1 presents the method to audit DP in a substitute-adjacency threat model.

136 3.1 AUDITING MODELS
137 USING CRAFTED WORST-CASE
138 DATASET CANARIES
139

140 DP gives an upper bound on privacy loss of an algorithm. It assumes that the adversary can access
141 the gradients from the mechanism. Furthermore, it guarantees that the privacy of a target record (crafted
142 to yield worst-case gradient) holds even when the adversary constructs a worst-case pair of neighbouring
143 datasets ($\mathcal{D}, \mathcal{D}'$). Thus, any privacy auditing procedure with such a strong adversary yields tightest empirical lower bound on privacy
144 parameters. Nasr et al. (2021) were the first to propose an auditing procedure which is provably
145 tight for worst-case neighbouring datasets crafted to audit DP with add/remove adjacency.

Algorithm 1 Privacy Auditing With Substitute Adjacency

Requires: Model Architecture \mathbb{M} , Model Initialization θ_0 , Dataset \mathcal{D} , Target Sample \mathbf{z} , Training Loss ℓ , Training Steps T , learning rate η , Optimizer `opt_step()`, Crafting Algorithm `craft()`, DP Parameters (σ, C, q) , Repeats R , Crafting $\in \{\text{Gradient-Space, Input-Space}\}$.

```

1:  $\mathcal{O} \leftarrow \mathbf{0}_R, \mathcal{B} \leftarrow \mathbf{0}_R$ 
   ▷ Adversary as Crafter:
2: if Crafting = Gradient-Space then
3:    $\mathbf{g}_z, \mathbf{g}_{z'} \leftarrow \text{craft}(\mathbb{M}, \mathcal{D}, \theta_0, T, \eta, \ell, C, q, \text{opt\_step})$ 
4: else
5:    $\mathbf{z}' \leftarrow \text{craft}(\mathbf{z}, \mathbb{M}, \mathcal{D}, \theta_0, T, \eta, \ell, \text{opt\_step})$ 
6: for  $r \in 1, \dots, R$  do
   ▷ Challenger as Model Trainer:
7:   Choose  $b$  uniformly at random:  $b \sim \{0, 1\}$ 
8:    $\mathcal{B}[r] \leftarrow b$ 
9:   for  $t \in 1, \dots, T$  do
10:    Sample  $B_t$  from  $\mathcal{D}$  with prob.  $q$ 
11:     $g_{\theta_t} \leftarrow \mathbf{0}_{|\theta|}$ 
12:    for  $z_i \in B_t$  do
13:       $g_{\theta_t} \leftarrow g_{\theta_t} + \text{clip}(\nabla_{\theta}(\ell(z_i), C)$ 
14:    if  $b = 0$  then
15:       $g_{\theta_t} \leftarrow g_{\theta_t} + [\text{clip}(\nabla_{\theta}(\ell(\theta_t; \mathbf{z}), C) \text{ or } +\mathbf{g}_z)]$  with prob.  $q$ 
16:    else
17:       $g_{\theta_t} \leftarrow g_{\theta_t} + [\text{clip}(\nabla_{\theta}(\ell(\theta_t; \mathbf{z}'), C) \text{ or } +\mathbf{g}_{z'})]$  with prob.  $q$ 
18:     $g_{\theta_t} \leftarrow g_{\theta_t} + \mathcal{N}(0, \sigma^2 C^2 \mathbb{I})$ 
19:     $\theta_{t+1} \leftarrow \text{opt\_step}(\theta_t, g_{\theta_t}, \eta)$ 
   ▷ Adversary as Distinguisher:
20:    $\mathcal{O}[r] \leftarrow \text{logit}(\mathbf{z}; \theta_T) - \text{logit}(\mathbf{z}'; \theta_T) \text{ or } \left( \frac{\mathbf{g}_z}{C} \right) \cdot (\theta_T - \theta_0)$ 
21: return  $\mathcal{O}, \mathcal{B}$ 

```

162
 163
 164
 165
 166
 167
 168
 169
 170
 171
 172
 173
 174
 175
 176
 177
 178
 179
 180
 181
 182
 183
 184
 185
 186
 187
 188
 189
 190
 191
 192
 193
 194
 195
 196
 197
 198
 199
 200
 201
 202
 203
 204
 205
 206
 207
 208
 209
 210
 211
 212
 213
 214
 215

Table 1: Crafting schema for auditing privacy leakage under substitute adjacency with varying adversary capabilities. The adversary can either craft canaries that allow them to directly manipulating the gradient input to the DP algorithm or they are restricted to input-space perturbations to craft the canary samples. **The adversary’s visibility into the training process is defined by the following threat models:** (a) Visible-State (commonly referred to in the literature as White-Box), where the adversary assumes access to gradients from the model, and (b) Hidden-State, where they rely on model parameter updates/ output logits to estimate privacy loss.

Scenario	Crafting Space	Type of Canary	Crafting Algorithm	Distinguishability Score	Threat Model
S1	Gradient	Crafted Dataset	Section 3.1	$\log(\Pr(g_T \mathcal{D})) - \log(\Pr(g_T \mathcal{D}'))$	Visible-State
S2	Gradient	Crafted Gradient	Algorithm 2	$\theta_T - \theta_0$	Hidden-State
S3	Input	Crafted Input Sample	Algorithm 3	$\text{logit}(z; \theta_T) - \text{logit}(z'; \theta_T)$	Hidden-State
S4	Input	Crafted Mislabeled Sample	Algorithm 4	$\text{logit}(z; \theta_T) - \text{logit}(z'; \theta_T)$	Hidden-State
S5	Input	Adversarial Natural Sample	Algorithm 5	$\text{logit}(z; \theta_T) - \text{logit}(z'; \theta_T)$	Hidden-State

We craft \mathcal{D} and \mathcal{D}' as worst-case neighbouring datasets under substitute adjacency (see **scenario S1 in Table 1**). Assuming \mathcal{D} has a sample z which yields a gradient g_z such that $\|g_z\| = C$ throughout training. For maximum distinguishability, we form \mathcal{D}' by replacing z with z' such that $\|g_{z'}\| = C$ but it is directionally opposite to g_z . For all the other samples in \mathcal{D} and \mathcal{D}' , we assume that they contribute 0 gradients during training. Unlike Nasr et al. (2021), we do not assume that the learning rate is 0 for the steps with no gradient canary in the minibatch since this discounts the effect of subsampling on auditing. Since we account for the noise contribution by the minibatches without z or z' , our setting more accurately reflects the true dynamics of DP-SGD. We further assume the adversary cannot access intermediate updates and observes only the final gradients from the mechanism.

At any step T , given subsampling rate q , the number of times the canary is sampled over T steps is a binomial, $\mathcal{B} \sim \text{Binomial}(T, q)$. Conditioned on $\mathcal{B} = k$, the cumulative gradient g_T given by

$$\Pr(g_T|\mathcal{B} = k) \sim \mathcal{N}(\pm kC, T\sigma^2C^2). \quad (2)$$

The marginal distribution of g_T over \mathcal{D} or \mathcal{D}' at step T is given by

$$\Pr(g_T|\mathcal{D} \text{ or } \mathcal{D}') = \sum_{k=0}^T \binom{T}{k} q^k (1-q)^{T-k} \mathcal{N}(g_T; \pm kC, T\sigma^2C^2), \quad (3)$$

where C is the gradient contribution of \mathcal{D} and $-C$ of \mathcal{D}' . The adversary can use Equation (3) to compute $\log(\Pr(g_T|\mathcal{D})) - \log(\Pr(g_T|\mathcal{D}'))$ as the scores to compute the empirical lower bound for ε_S during auditing.

3.2 AUDITING MODELS TRAINED WITH NATURAL DATASETS

While DP offers protection to training samples against worst-case adversaries, high-utility ML models are obtained by training on natural datasets. Under substitute adjacency, \mathcal{D} and \mathcal{D}' differ by replacing a target sample z in \mathcal{D} with z' . Effective auditing for models trained with natural datasets, therefore requires canaries that maximize the distinguishability between the two datasets.

3.2.1 CRAFTING CANARIES FOR AUDITING IN GRADIENT SPACE

Recently, Cebere et al. (2025) propose a worst-case gradient canary for tight auditing on models trained with add/remove DP using natural datasets in a hidden state threat model. Adapting their idea to substitute adjacency-based auditing, we first select the trainable model parameter which changes least in terms of its magnitude throughout training.

216 We then define canary gradients g_z and $g_{z'}$ by setting all other parameter gradients to
 217 0, and assigning a magnitude C to the gradient of the selected least-updated parameter.
 218 This ensures that $\|g_z\| = \|g_{z'}\| = C$. For maximum distinguishability between g_z and $g_{z'}$, we
 219 orient them in opposite directions in gradient space. The detailed procedure for constructing
 220 these canaries is provided in Algorithm 2. For computing the empirical privacy leakage,
 221 we record change in parameter from initialization, $\theta_t - \theta_0$ as scores for auditing. These
 222 scores serve as proxies for the adversary’s confidence that the observed outputs were from
 223 model trained on \mathcal{D} or \mathcal{D}' . **This setting corresponds to scenario S2 in Table 1.** Such canaries
 224 can be used to audit models trained using federated learning.
 225

3.2.2 CRAFTING CANARIES FOR AUDITING IN INPUT SPACE

231 In practice, adversaries are unlikely to directly
 232 manipulate a model’s gradient space during
 233 training. In such cases, the adversary is constrained to input-space perturbations where a natural
 234 sample $z \in \mathcal{D}$ will be replaced with an adversarially crafted sample z' to form \mathcal{D}' prior to training.
 235 **For instance, an adversary could mount a data-poisoning attack during the fine-tuning of a large**
 236 **model, or attempt to infer the label of a known-in-training user.** For input-space canaries, we track
 237 $\text{logit}(z; \theta_t) - \text{logit}(z'; \theta_t)$ as scores for auditing.

238 For auditing using input-space canaries, we
 239 begin by selecting a target sample (z) for
 240 which the a reference model (trained with-
 241 out DP) exhibits least-confidence over train-
 242 ing. The crafted canary equivalent (z') can
 243 then be generated using the following crite-
 244 ria:

- 245 • Algorithm 3 is used to generate a *crafted input* canary $z' \sim (x', y)$ complementary to the target sample z (**Scenario S3 in Table 1**). It uses the reference model to craft z' such that the cosine similarity between g_z and $g_{z'}$ is minimized while ensuring that $g_{z'}$ is similar in scale to g_z so that the model interprets z' as a legitimate sample from the data distribution.
- 246 • Algorithm 4 is used to generate a *crafted mislabeled* canary $z' \sim (x, y')$ complementary to the target sample z (**Scenario S4 in Table 1**). We use the reference model to find a label y' in the label space \mathcal{Y} such that it minimizes cosine similarity between $g_{z'}$ and $g_{z'}$.
- 247 • Algorithm 5 is used to select an *adversarial natural* canary $z' \sim (x', y')$ from an auxiliary dataset \mathcal{D}_{aux} (formed using a subset of samples not used for training the model) complementary to the target sample z (**Scenario S5 in Table 1**). We use the reference model to find a sample z' in \mathcal{D}_{aux} which yields minimum cosine similarity between $g_{z'}$ and $g_{z'}$.

4 USE OF GROUP PRIVACY TO APPROXIMATE SUBSTITUTE ADJACENCY YIELDS SUBOPTIMAL UPPER BOUNDS

265 By the definition of DP with substitute adjacency (Definition 1), \mathcal{D}' can be obtained from \mathcal{D} by
 266 removing a record z and adding another record z' to \mathcal{D} . As such, it is a common practice to infer
 267

Algorithm 2 Generating Crafted Gradient Canary Pair $(g_z, g_{z'})$

Requires: Dataset \mathcal{D} , Training Loss ℓ , Model Initialization θ_0 , Training Steps T , Learning Rate η , Clipping Bound C , Optimizer $\text{opt_step}()$.

```

1: def craft:
2:    $S \leftarrow \mathbf{0}_d$  s.t.  $d \leftarrow |\theta_0|$ 
3:   for  $t \in 1, \dots, T$  do
4:     Sample  $B_t$  from  $\mathcal{D}$ 
5:      $\bar{g}_{\theta_t} \leftarrow \text{clip}(\nabla_{\theta} \ell(\theta_t; z_t), C)$ 
6:      $\theta_{t+1} \leftarrow \text{opt\_step}(\theta_t, \bar{g}_{\theta_t}, \eta)$ 
7:     for  $j \in 1, \dots, d$  do
8:        $S_j \leftarrow S_j + |\theta_{t+1}^j - \theta_t^j|$ 
9:      $j^* \leftarrow \text{argmin}_{1 \leq j \leq d}(S_j)$ 
10:     $g_z \leftarrow \mathbf{0}_d$ 
11:     $g_z[j^*] \leftarrow C$ 
12:     $g_{z'} \leftarrow \mathbf{0}_d$ 
13:     $g_{z'}[j^*] \leftarrow -C$ 
14:   return  $g_z, g_{z'}$ 

```

Algorithm 3 Generating Crafted Input Canary $(z' \sim (x', y))$

Requires: Target Sample $z \sim (x, y)$, Dataset \mathcal{D} , Training Loss ℓ , Model \mathbb{M} , Model Initialization θ_0 , Training Steps T , Crafting Steps N , Learning Rate η .

```

1: def craft:
2:    $\theta_T \leftarrow \text{train}(\mathbb{M}, \theta_0, \mathcal{D}, T, \ell, \eta)$ 
3:    $z' \sim (x', y)$  s.t.  $x' \leftarrow \mathbf{0}_{|x|}$ 
4:    $\mathcal{L}_{\text{cosim}}(x') \leftarrow \frac{\nabla_{\theta} \ell(\theta_T; x, y) \cdot \nabla_{\theta} \ell(\theta_T; x', y)}{\|\nabla_{\theta} \ell(\theta_T; x, y)\| \cdot \|\nabla_{\theta} \ell(\theta_T; x', y)\|}$ 
5:    $\mathcal{L}_{\text{MSE}}(x') \leftarrow \text{MSE}(\nabla_{\theta} \ell(\theta_T; x, y), \nabla_{\theta} \ell(\theta_T; x', y))$ 
6:   for  $n \in 1, \dots, N$  do
7:      $x' \leftarrow x' - \eta(\nabla \mathcal{L}_{\text{cosim}}(x') + \nabla \mathcal{L}_{\text{MSE}}(x'))$ 
8:   return  $z'$ 

```

270 Substitute adjacency as a composition of one Add and one Remove operation (Kulesza et al., 2024).
 271 According to Dwork & Roth (2014), if an algorithm \mathcal{M} satisfies $(\varepsilon, \delta, \sim_{AR})$ -DP, then for any pair
 272 of \mathcal{D} and \mathcal{D}' that differ in at most k records, the following relationship holds true
 273

$$\Pr[\mathcal{M}(\mathcal{D}) \in S] \leq e^{k\varepsilon} \Pr[\mathcal{M}(\mathcal{D}') \in S] + \left(\sum_{i=0}^{k-1} e^{i\varepsilon} \right) \delta. \quad (4)$$

277 From Equation (4), it follows that
 278

279 **Theorem 4.1** (Dwork & Roth (2014)). *Any algorithm \mathcal{M} which satisfies $(\varepsilon_{AR}, \delta_{AR}, \sim_{AR})$ -DP is
 280 $(\varepsilon_S, \delta_S, \sim_S)$ -DP with $\varepsilon_S = 2\varepsilon_{AR}$ and $\delta_S = (1 + e^{\varepsilon_{AR}})\delta_{AR}$.*

281 Theorem 4.1 yields an upper bound for substitute DP derived from add/remove DP which is agnostic
 282 of the underlying algorithm. For certain algorithms (such as the Poisson-subsampled DP-SGD used
 283 in this paper), which can be characterized by privacy loss random variables (PRVs) and their corre-
 284 sponding privacy loss distribution (PLD) (Dwork & Rothblum, 2016; Meiser & Mohammadi, 2018;
 285 Koskela et al., 2020), numerical accountants can derive the privacy curve directly. This approach
 286 is recommended over using general, algorithm-agnostic upper bounds, as it provides significantly
 287 tighter privacy guarantees.

288 **Algorithm 4** Generating Crafted Mislabeled
 289 Canary ($z' \sim (x, y')$)
 290

291 **Requires:** Target Sample $z \sim (x, y)$, Dataset \mathcal{D} ,
 292 Training Loss ℓ , Model \mathbb{M} , Model Initialization θ_0 ,
 293 Training Steps T , Learning Rate η , Label Space \mathcal{Y} .

```

1: def craft:
2:    $\theta_T \leftarrow \text{train}(\mathbb{M}, \theta_0, \mathcal{D}, T, \ell, \eta)$ 
3:    $S \leftarrow \mathbf{0}_d$  s.t.  $d \leftarrow |\mathcal{Y}|$ 
4:   for  $\hat{y} \in \mathcal{Y}$  do
5:      $\hat{z} \sim (x, \hat{y})$ 
6:      $S[\hat{y}] \leftarrow \frac{\nabla_{\theta}\ell(\theta_T; z)\nabla_{\theta}\ell(\theta_T; \hat{z})}{\|\nabla_{\theta}\ell(\theta_T; z)\|\|\nabla_{\theta}\ell(\theta_T; \hat{z})\|}$ 
7:      $j^* \leftarrow \text{argmin}_{1 \leq j \leq d}(S_j)$ 
8:      $y' \leftarrow \mathcal{Y}[j^*]$ 
9:   return  $z'$ 
```

288 **Algorithm 5** Selecting Canary From Natural
 289 Samples ($z' \sim (x', y')$)
 290

291 **Requires:** Target Sample $z \sim (x, y)$, Dataset \mathcal{D} , Training Loss ℓ , Model \mathbb{M} , Model Initialization θ_0 , Training Steps T , Learning Rate η , Auxiliary Dataset \mathcal{D}_{aux} .

```

1: def craft:
2:    $\theta_T \leftarrow \text{train}(\mathbb{M}, \theta_0, \mathcal{D}, T, \ell, \eta)$ 
3:    $S \leftarrow \mathbf{0}_d$  s.t.  $d \leftarrow |\mathcal{D}_{\text{aux}}|$ 
4:   for  $\hat{z} \in \mathcal{D}_{\text{aux}}$  do
5:      $\hat{z} \sim (\hat{x}, \hat{y})$ 
6:      $S[\hat{z}] \leftarrow \frac{\nabla_{\theta}\ell(\theta_T; z)\nabla_{\theta}\ell(\theta_T; \hat{z})}{\|\nabla_{\theta}\ell(\theta_T; z)\|\|\nabla_{\theta}\ell(\theta_T; \hat{z})\|}$ 
7:      $j^* \leftarrow \text{argmin}_{1 \leq j \leq d}(S_j)$ 
8:      $z' \leftarrow \mathcal{D}_{\text{aux}}[j^*]$ 
9:   return  $z'$ 
```

303 **5 GENERAL EXPERIMENTAL SETTINGS**

304 **Training Details:**

- 307 **Training Paradigm:** We fine-tune the final layer of ViT-B-16 (Dosovitskiy et al., 2021)
 308 model pretrained on ImageNet21K. **We also fine-tune a linear layer on top of Sentence-BERT**
 309 **(Reimers & Gurevych, 2019) encoder for text classification experiments.** We use a 3-layer
 310 fully-connected multi-layer perceptron (MLP) (Shokri et al., 2017) for the from-scratch train-
 311 ing experiments.
- 312 **Datasets:** For supervised fine-tuning experiments, we use 500 samples from CIFAR10
 313 (Krizhevsky, 2009), a widely used benchmark for image classification tasks (De et al., 2022;
 314 Tobaben et al., 2023) **and 5K samples from SST-2 (Socher et al., 2013) for text classification**
 315 **task.** To train models from scratch, we use 50K samples from Purchase100 (Shokri et al., 2017).
- 316 **Privacy Accounting:** We adapt Microsoft’s `prv-accountant` (Gopi et al., 2021) to com-
 317 pute the theoretical upper bounds for substitute adjacency-based DP with Poisson subsampling.
 318 We share the code for this accountant in supplementary materials.
- 319 **Hyperparameters:** We tune the noise added for DP relative to the subsampling rate q and train-
 320 ing steps T . We keep the other training hyperparameters fixed to isolate the effect of privacy
 321 amplification by subsampling (Bassily et al., 2014; Balle et al., 2018) on auditing performance.
 322 Detailed description of the hyperparameters used in our experiments is provided in Table A1.
- 323 **Auditing Privacy Leakage / Step:** We perform step-wise audits by treating the model at each
 324 training step t as a provisional model released to the adversary. The adversary is restricted to use
 325 only current model’s parameters or outputs to compute the empirical privacy leakage at step t .

324 **Computing Empirical ε with Gaussian DP (Dong et al., 2019):** DP (by Definition 1) implies an
 325 upper bound on the adversary’s capability to distinguish between $\mathcal{M}(\mathcal{D})$ and $\mathcal{M}(\mathcal{D}')$. For computing
 326 the corresponding empirical lower bound on ε , we use the method prescribed by Nasr et al. (2023)
 327 which relies on μ -GDP. This method allows us to get a high confidence estimate of ε with reasonable
 328 repeats of the training algorithm.

329 Given a set of observations \mathcal{O} and corresponding ground truth labels \mathcal{B} obtained from Algorithm 1,
 330 the auditor can compute the False Negatives (FN), False Positives (FP), True Negatives (TN),
 331 and True Positives (TP) at a fixed threshold. Using these measures, the auditor estimates upper
 332 bounds on the false positive rate ($\overline{\text{FPR}}$) and false negative rate ($\overline{\text{FNR}}$) by using the Clopper–Pearson
 333 method (Clopper & Pearson, 1934) with significance level $\alpha = 0.05$.

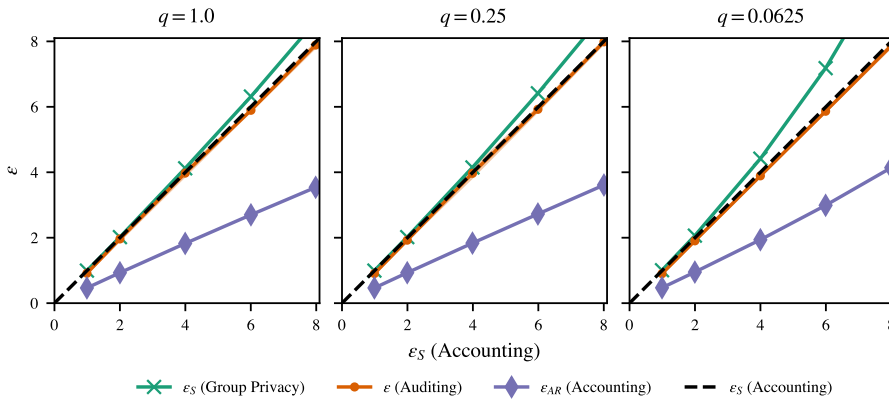
334 Kairouz et al. (2015) express privacy region of a DP algorithm in terms of FPR and FNR. DP
 335 bounds the FPR and FNR attainable by any adversary. Nasr et al. (2023) note that the privacy
 336 region for DP-SGD can be characterized by μ -GDP (Dong et al., 2019). Thus, the auditor can use
 337 $\overline{\text{FPR}}$ and $\overline{\text{FNR}}$ to compute the corresponding empirical lower bound on μ in μ -GDP,
 338

$$\mu_{\text{lower}} = \Phi^{-1}(1 - \overline{\text{FPR}}) - \Phi^{-1}(\overline{\text{FNR}}), \quad (5)$$

339 where Φ represents the cumulative density function of standard normal distribution $\mathcal{N}(0, 1)$. This
 340 lower bound on μ can be translated into a lower bound on ε given a δ in (ε, δ) -DP using the following
 341 theorem,

342 **Theorem 5.1** (Dong et al. (2019) Conversion from μ -GDP to (ε, δ) -DP. *If a mechanism \mathcal{M} is*
 343 *μ -GDP, then it is also (ε, δ) -DP ($\varepsilon \geq 0$), where*

$$\delta(\varepsilon) = \Phi\left(-\frac{\varepsilon}{\mu} + \frac{\mu}{2}\right) - e^{\varepsilon}\Phi\left(-\frac{\varepsilon}{\mu} - \frac{\mu}{2}\right). \quad (6)$$



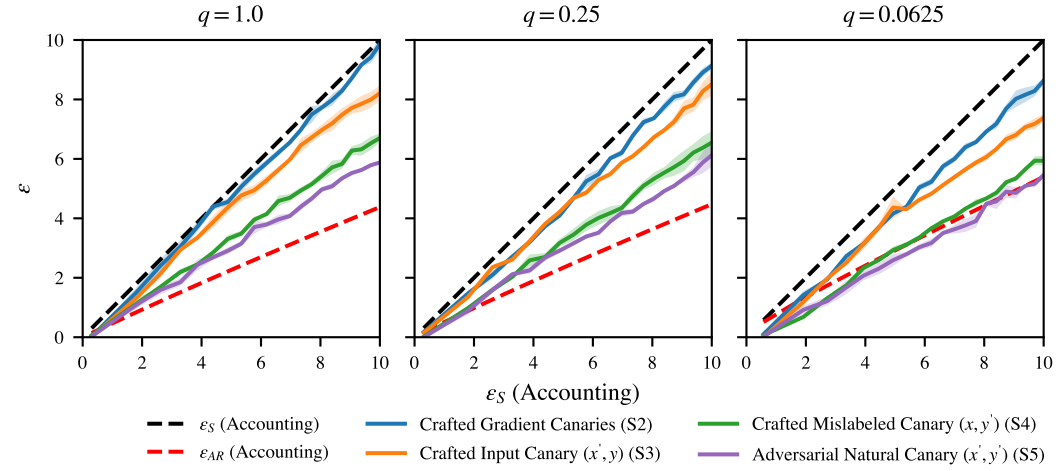
362 **Figure 1: Auditing DP using worst-case dataset canaries based on substitute adjacency.** When
 363 the adversary crafts the neighbouring datasets as worst-case dataset canaries (S1), we find that the
 364 empirical privacy leakage for a DP algorithm, ε (Auditing), exceeds the privacy upper bound for
 365 add/remove DP, ε_{AR} (Accounting). It closely tracks the privacy budget predicted by substitute
 366 accountant, ε_S (Accounting). The plot shows that ε_S (Accounting) is tighter when compared to that
 367 ε_S (Group Privacy) computed using Theorem 4.1. We fix $\delta_{\text{target}} = 10^{-5}$, $C = 1.0$ and $T = 500$. The
 368 auditing estimates are averaged over 3 repeats. For each repeat, we use $R = 25K$ runs to estimate ε
 369 (Auditing) at the final step of training. **The error bars represent ± 2 standard errors around the mean**
 370 **computed over 3 repeats of auditing algorithm.**

6 RESULTS

6.1 AUDITING WITH WORST-CASE CRAFTED DATASET CANARIES

371 Figure 1 depicts the relation between ε_S (Accounting) computed with a substitute accountant, ε_S
 372 (Group Privacy) computed using Theorem 4.1, ε (Auditing) using crafted worst-case dataset
 373 canaries from Section 3.1, and ε_{AR} (Accounting) computed with an add/remove accountant for a set
 374 of DP parameters. We observe that ε (Auditing) exceeds ε_{AR} (Accounting) but remains tight with

378 respect to ε_S (Accounting). Thus, mounting a substitute-style attack using worst-case dataset
 379 canaries enables the adversary to detect whether \mathcal{D} or \mathcal{D}' was used for training a model with higher
 380 confidence than promised by ε_{AR} (Accounting).



398 **Figure 2: Auditing models trained with DP using natural datasets.** We fine-tune final layer of
 399 ViT-B-16 models pretrained on ImageNet21K using CIFAR10. The privacy leakage (ε) audited using
 400 our proposed canaries for this setting exceeds the add/remove DP upper bounds, ε_{AR} (Accounting). As these
 401 canaries are used to mount a substitute-style attack, the figure shows that add/remove
 402 DP overestimates protection against such attacks. Efficacy of the canaries decline as subsampling
 403 rate q decreases, the effect being most significant for audits using input-space canaries. We plot ε
 404 for every k th step ($k = 25$) of training averaged over 3 repeats of the auditing algorithm. For each
 405 repeat, we train $R = 2500$ models, $1/2$ trained with z and the remaining with z' . **The error bars**
 406 **represent ± 2 standard errors around the mean computed over 3 repeats of auditing algorithm.**

407 6.2 AUDITING MODELS TRAINED WITH NATURAL DATASETS

409 In this section, we report auditing results on models trained with natural datasets. In fine-tuning
 410 experiments with CIFAR10, all proposed canaries outperform add/remove DP at large subsampling
 411 rates. With the strongest canaries, we observe that the empirical privacy leakage exceeds the
 412 add/remove DP upper bounds for models trained from scratch with Purchase100.

414 6.2.1 USING GRADIENT-SPACE CANARIES

416 Figure 2 shows that, when auditing models that are trained using natural datasets, we get the tightest
 417 estimates of ε by using crafted gradient canaries for auditing. The empirical privacy leakage (ε)
 418 estimated using these canaries violates ε_{AR} (Accounting). The canary gradients, g_z and $g_{z'}$, crafted
 419 using Algorithm 2 stay constant over the course of training and have near-saturation gradient norms
 420 ($\|g_z\| = \|g_{z'}\| = C$). This ensures that their effect on the parameter updates of the model is
 421 consistent and is most affected by the choice of subsampling rate q . As q decreases, the canary is
 422 less visible to the model during training, which yields weaker audits.

423 6.2.2 USING INPUT-SPACE CANARIES

425 In this setting, the adversary is only permitted to insert a crafted input record into the training dataset.
 426 In Figure 2, we observe that even though input-space canaries yield less tight audits when compared
 427 to crafted gradient canaries, the privacy leakage audited using the input-space canaries can exceed
 428 the guarantees of add/remove DP. We observe that the efficacy of audits with input-space canaries
 429 decreases for later training steps. This deterioration is much more significant at a low subsampling
 430 rate (q). Additionally, in Appendix A.2, we observe that audits using input-space canaries are
 431 sensitive to the choice of other training hyperparameters such as the number of training steps T , clipping
 bound C , and the learning rate η .

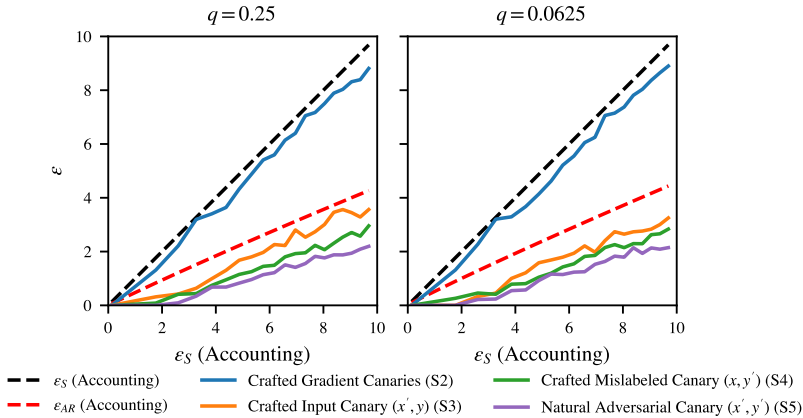


Figure 3: **Auditing MLP model trained from scratch with random initialization using Purchase100.** We find that auditing such models using input-space canaries yield weaker audits. We do not observe ϵ from such audits to exceed the privacy implied by ϵ_{AR} (Accounting). However, using crafted gradient canaries, we still get ϵ from auditing which is consistent with ϵ_S (Accounting). We plot ϵ for every k th step ($k = 125$) of training. We train $R = 2500$ models, $1/2$ trained with z and the remaining with z' .

6.2.3 AUDITING MODELS TRAINED FROM SCRATCH

Training models from scratch with random initialization is a non-convex optimization problem. Figure 3 shows that auditing models trained from scratch on Purchase100 dataset using input-space canaries yields weaker audits. We find that input-space canaries are sensitive to model initialization and the choice of optimizer (DP-Adam in this case). Subsampling further deteriorates the effectiveness of audits with input-space canaries. In this setting, add/remove DP does suffice to protect against attacks using input-space canaries as shown in Figure 3. However, our proposed crafted gradient canaries still yield strong audits for models trained from scratch with empirical privacy leakage that closely follows ϵ_S (Accounting).

6.3 AUDITING MODELS FINE-TUNED FOR TEXT CLASSIFICATION

We fine-tune a linear layer on top of Sentence-BERT (Reimers & Gurevych, 2019) encoder using 5K samples from Stanford’s Sentiment Treebank (SST-2) dataset (Socher et al., 2013). We present the results for this experiment in Figure A6. The models are trained using DP-SGD. We find that gradient-canary-based auditing yields tight results. While the audits using input-space canaries are not tight, we do observe that the empirical privacy leakage estimated using them does exceed the privacy guaranteed by add/remove DP.

7 DISCUSSION AND CONCLUSION

We provide empirical evidence which shows that for certain ML models, DP with add/remove adjacency will not offer adequate protection against attacks such as attribute inference at the level guaranteed by the privacy parameters. This is because the threat model for these attacks mimics substitute-style attacks. In Figure 2, for DP models are trained using natural datasets, we observe violations of add/remove DP guarantees with the canaries designed to substitute a target record or a target record’s gradient in the training dataset. The resulting empirical privacy leakage from such audits closely follows DP upper bound for substitute adjacency. Thus, practitioners seeking attribute or label privacy using standard DP libraries which default to add/remove adjacency-based accountants might risk overestimating the protection add/remove DP affords against substitute-style attacks.

We observe that fine-tuned models (as shown in Figure 2) are more prone to privacy leakage with input-space canaries compared to models trained from scratch (Figure 3). In practice, limited sensitive data makes DP training from scratch challenging. Tramèr & Boneh (2021) have shown that given a suitable public pretraining dataset, fine-tuning a pretrained model on sensitive data can yield higher utility than models trained from scratch. This makes our results with supervised

486 fine-tuning important since it reveals that poisoning the fine-tuning datasets once with input-space
 487 canaries is sufficient to cause privacy leakage exceeding add/remove DP bounds, particularly at
 488 large subsampling rates which are often used for improved privacy–utility trade-off (De et al., 2022;
 489 Mehta et al., 2023).

490

491

492

493

494

495

496

497

498

499

500

501

502

503

504

505

506

507

508 **Figure 4: Effect of number of training runs R on privacy auditing.** For ViT-B-16 models with
 509 final layer fine-tuned on CIFAR10 ($T = 500, C = 2.0$), we record the effect of change in R on the
 510 empirical privacy leakage $\hat{\epsilon}$, at the final step of training. The error bars represent ± 2 standard errors
 511 around the mean computed over 3 repeats of auditing algorithm. In each repeat, 1/2 of the models
 512 are trained with z and the remaining with z' .

513

514

515

516 Our methods to audit DP under substitute adjacency are not without limitations. We note that the
 517 efficacy of our proposed input-space canaries depends strongly on the training hyperparameters (see
 518 Appendix A.2). They provide weaker audits at later training steps, especially when the training
 519 problem involves non-convex optimization and a low subsampling rate q . This has been a persistent
 520 issue with input-space canaries as noted by Nasr et al. (2023). Our results show that canaries with
 521 consistent gradient signals and near-saturation gradient norms are most robust to the effect of train-
 522 ing hyperparameters. An interesting direction for future work is to design input-space canaries that
 523 are robust to training hyperparameters and yield tight audits for models trained with real, non-convex
 524 objectives. Our canaries are tailored to audit gradient-based DP algorithms, such as DP-SGD. We
 525 expect the canaries to work well with other gradient-based methods, such as DP-Adam, although
 526 some performance degradation is possible (as seen in Figure 3). However, we do not expect our pro-
 527 posed auditing approach to extend to other DP mechanisms which operate differently. For instance,
 528 label DP (Chaudhuri & Hsu, 2011) is a special case of substitute DP, where you only substitute the
 529 label of an example. Auditing using a crafted mislabeled canary is the same threat model as label
 530 DP. As substitute DP is a generalization of label DP, it will also be valid for auditing a substitute
 531 DP mechanism, even though it might not be optimal for that. While DP-SGD with substitute ac-
 532 counting is a valid label DP mechanism, in practice, label DP is implemented using very different
 533 methods (Ghazi et al., 2021; 2024; Busa-Fekete et al., 2023; Zhao et al., 2025). As such, our auditing
 534 techniques would not be suitable for those methods.

535

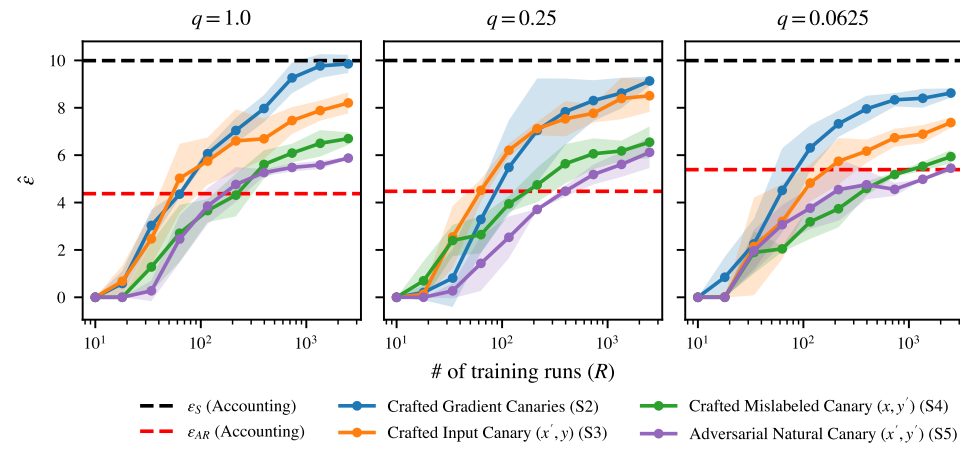
536

537

538

539

540 Furthermore, our methods for privacy auditing rely on multiple repeats of the training process to
 541 obtain a high confidence measure of lower bound on ϵ . In Figure 4, we observe that with limited
 542 number of runs, there is a risk of underestimating the privacy leakage. At low subsampling rate (q),
 543 the continuous upward trend of auditing curves show that the process has not converged, even with
 544 $R = 2500$ runs. While the current method is costly, it could potentially be optimized by integrating
 545 our proposed canaries with some recent works on auditing using single training run (Steinke et al.,
 546 2023; Mahloujifar et al., 2025). However, as these works note, this might involve a trade-off between
 547 computational efficiency and the strength of the resulting audits.



540 REPRODUCIBILITY STATEMENT
541542 The code for our experiments in Section 6 is available at: https://anonymous.4open.science/r/auditing_substitute_relation-016B. We adapt the code from Tobaben et al. (2023) for the fine-tuning experiments.
543
544546 ETHICS STATEMENT
547548 The research conducted in the paper conform, in every respect, with the ICLR Code of Ethics
549 (<https://iclr.cc/public/CodeOfEthics>).
550
551552 USE OF LARGE LANGUAGE MODELS (LLMS)
553554 We used LLMs to polish the content of this manuscript for readability and conciseness. We also
555 used it to improve the presentation of mathematical content with LaTeX. LLMS were not used to
556 generate any novel content.
557558 REFERENCES
559560 Martín Abadi, Andy Chu, Ian J. Goodfellow, H. Brendan McMahan, Ilya Mironov, Kunal Talwar,
561 and Li Zhang. Deep Learning with Differential Privacy. In *Proceedings of the 2016 ACM SIGSAC*
562 *Conference on Computer and Communications Security*, pp. 308–318. ACM, 2016.563 Meenatchi Sundaram Muthu Selva Annamalai. It’s Our Loss: No Privacy Amplification for Hidden
564 State DP-SGD With Non-Convex Loss. In Maura Pintor, Xinyun Chen, and Matthew Jagielski
565 (eds.), *Proceedings of the 2024 Workshop on Artificial Intelligence and Security, AISec 2024, Salt*
566 *Lake City, UT, USA, October 14-18, 2024*, pp. 24–30. ACM, 2024.567 Meenatchi Sundaram Muthu Selva Annamalai and Emilio De Cristofaro. Nearly Tight Black-
568 Box Auditing of Differentially Private Machine Learning. In Amir Globersons, Lester Mackey,
569 Danielle Belgrave, Angela Fan, Ulrich Paquet, Jakub M. Tomczak, and Cheng Zhang (eds.), *Ad-*
570 *vances in Neural Information Processing Systems 38: Annual Conference on Neural Information*
571 *Processing Systems 2024, NeurIPS 2024, Vancouver, BC, Canada, December 10 - 15, 2024*, 2024.572 Borja Balle, Gilles Barthe, and Marco Gaboardi. Privacy Amplification by Subsampling: Tight
573 Analyses via Couplings and Divergences. In Samy Bengio, Hanna M. Wallach, Hugo Larochelle,
574 Kristen Grauman, Nicolò Cesa-Bianchi, and Roman Garnett (eds.), *Advances in Neural Infor-*
575 *mation Processing Systems 31: Annual Conference on Neural Information Processing Systems 2018,*
576 *NeurIPS 2018, December 3-8, 2018, Montréal, Canada*, pp. 6280–6290, 2018.577 Raef Bassily, Adam D. Smith, and Abhradeep Thakurta. Private Empirical Risk Minimization:
578 Efficient Algorithms and Tight Error Bounds. In *55th IEEE Annual Symposium on Foundations*
579 *of Computer Science, FOCS 2014, Philadelphia, PA, USA, October 18-21, 2014*, pp. 464–473.
580 IEEE Computer Society, 2014.581 Matteo Bogioni, Terrance Liu, Andrew Ilyas, and Zhiwei Steven Wu. Optimizing Canaries for
582 Privacy Auditing with Metagradient Descent. *CoRR*, abs/2507.15836, 2025.583 Mark Bun and Thomas Steinke. Concentrated Differential Privacy: Simplifications, Extensions, and
584 Lower Bounds. In Martin Hirt and Adam D. Smith (eds.), *Theory of Cryptography - 14th Inter-*
585 *national Conference, TCC 2016-B, Beijing, China, October 31 - November 3, 2016, Proceedings,*
586 *Part I*, volume 9985 of *Lecture Notes in Computer Science*, pp. 635–658, 2016.587 Róbert Istvan Busa-Fekete, Andrés Muñoz Medina, Umar Syed, and Sergei Vassilvitskii. La-
588 bel differential privacy and private training data release. In Andreas Krause, Emma Brunskill,
589 Kyunghyun Cho, Barbara Engelhardt, Sivan Sabato, and Jonathan Scarlett (eds.), *International*
590 *Conference on Machine Learning, ICML 2023, 23-29 July 2023, Honolulu, Hawaii, USA*, volume
591 202 of *Proceedings of Machine Learning Research*, pp. 3233–3251. PMLR, 2023.

594 Tudor Ioan Cebere, Aurélien Bellet, and Nicolas Papernot. Tighter Privacy Auditing of DP-SGD in
 595 the Hidden State Threat Model. In *The Thirteenth International Conference on Learning Repre-*
 596 *sentations, ICLR 2025, Singapore, April 24-28, 2025*. OpenReview.net, 2025.

597

598 Kamalika Chaudhuri and Daniel J. Hsu. Sample complexity bounds for differentially private learn-
 599 ing. In Sham M. Kakade and Ulrike von Luxburg (eds.), *COLT 2011 - The 24th Annual Confer-
 600 ence on Learning Theory, June 9-11, 2011, Budapest, Hungary*, volume 19 of *JMLR Proceedings*,
 601 pp. 155–186. JMLR.org, 2011.

602 C. J. Clopper and E. S. Pearson. The Use of Confidence or Fiducial Limits Illustrated in the Case of
 603 the Binomial. *Biometrika*, 26(4):404–413, 12 1934. ISSN 0006-3444.

604

605 Soham De, Leonard Berrada, Jamie Hayes, Samuel L. Smith, and Borja Balle. Unlocking High-
 606 accuracy Differentially Private Image Classification through Scale. *CoRR*, abs/2204.13650, 2022.

607

608 Jinshuo Dong, Aaron Roth, and Weijie J. Su. Gaussian Differential Privacy. *CoRR*, abs/1905.02383,
 609 2019.

610 Alexey Dosovitskiy, Lucas Beyer, Alexander Kolesnikov, Dirk Weissenborn, Xiaohua Zhai, Thomas
 611 Unterthiner, Mostafa Dehghani, Matthias Minderer, Georg Heigold, Sylvain Gelly, Jakob Uszkoreit,
 612 and Neil Houlsby. An Image is Worth 16x16 Words: Transformers for Image Recognition
 613 at Scale. In *9th International Conference on Learning Representations, ICLR 2021*. OpenRe-
 614 view.net, 2021.

615

616 Cynthia Dwork and Aaron Roth. The Algorithmic Foundations of Differential Privacy. *Found.
 617 Trends Theor. Comput. Sci.*, 9(3-4):211–407, 2014.

618

619 Cynthia Dwork and Guy N. Rothblum. Concentrated Differential Privacy. *CoRR*, abs/1603.01887,
 620 2016.

621

622 Cynthia Dwork, Frank McSherry, Kobbi Nissim, and Adam D. Smith. Calibrating Noise to Sen-
 623 sitivity in Private Data Analysis. In Shai Halevi and Tal Rabin (eds.), *Theory of Cryptography,
 624 Third Theory of Cryptography Conference, TCC 2006, New York, NY, USA, March 4-7, 2006,
 625 Proceedings*, volume 3876 of *Lecture Notes in Computer Science*, pp. 265–284. Springer, 2006.

626

627 Cynthia Dwork, Guy N. Rothblum, and Salil P. Vadhan. Boosting and Differential Privacy. In *51th
 628 Annual IEEE Symposium on Foundations of Computer Science, FOCS 2010, Las Vegas, Nevada,
 629 USA, October 23-26, 2010*, pp. 51–60. IEEE Computer Society, 2010.

630

631 Badih Ghazi, Noah Golowich, Ravi Kumar, Pasin Manurangsi, and Chiyuan Zhang. Deep learning
 632 with label differential privacy. In Marc’Aurelio Ranzato, Alina Beygelzimer, Yann N. Dauphin,
 633 Percy Liang, and Jennifer Wortman Vaughan (eds.), *Advances in Neural Information Processing
 634 Systems 34: Annual Conference on Neural Information Processing Systems 2021, NeurIPS 2021,
 December 6-14, 2021, virtual*, pp. 27131–27145, 2021.

635

636 Badih Ghazi, Yangsibo Huang, Pritish Kamath, Ravi Kumar, Pasin Manurangsi, and Chiyuan Zhang.
 637 Labeldp-pro: Learning with label differential privacy via projections. In *The Twelfth International
 638 Conference on Learning Representations, ICLR 2024, Vienna, Austria, May 7-11, 2024*. OpenRe-
 view.net, 2024.

639

640 Sivakanth Gopi, Yin Tat Lee, and Lukas Wutschitz. Numerical Composition of Differential Privacy.
 641 In Marc’Aurelio Ranzato, Alina Beygelzimer, Yann N. Dauphin, Percy Liang, and Jennifer Wort-
 642 man Vaughan (eds.), *Advances in Neural Information Processing Systems 34: Annual Conference
 643 on Neural Information Processing Systems 2021, NeurIPS 2021, December 6-14, 2021, virtual*,
 644 pp. 11631–11642, 2021.

645

646 Bargav Jayaraman and David Evans. Evaluating Differentially Private Machine Learning in Prac-
 647 tice. In Nadia Heninger and Patrick Traynor (eds.), *28th USENIX Security Symposium, USENIX
 648 Security 2019, Santa Clara, CA, USA, August 14-16, 2019*, pp. 1895–1912. USENIX Association,
 649 2019.

648 Peter Kairouz, Sewoong Oh, and Pramod Viswanath. The Composition Theorem for Differential
 649 Privacy. In Francis R. Bach and David M. Blei (eds.), *Proceedings of the 32nd International
 650 Conference on Machine Learning, ICML 2015, Lille, France, 6-11 July 2015*, volume 37 of *JMLR
 651 Workshop and Conference Proceedings*, pp. 1376–1385. JMLR.org, 2015.

652 Peter Kairouz, Brendan McMahan, Shuang Song, Om Thakkar, Abhradeep Thakurta, and Zheng
 653 Xu. Practical and Private (Deep) Learning Without Sampling or Shuffling. In Marina Meila
 654 and Tong Zhang (eds.), *Proceedings of the 38th International Conference on Machine Learning,
 655 ICML 2021, 18-24 July 2021, Virtual Event*, volume 139 of *Proceedings of Machine Learning
 656 Research*, pp. 5213–5225. PMLR, 2021.

657 Diederik P. Kingma and Jimmy Ba. Adam: A Method for Stochastic Optimization. In Yoshua
 658 Bengio and Yann LeCun (eds.), *3rd International Conference on Learning Representations, ICLR
 659 2015, San Diego, CA, USA, May 7-9, 2015, Conference Track Proceedings*, 2015.

660 Antti Koskela, Joonas Jälkö, and Antti Honkela. Computing Tight Differential Privacy Guarantees
 661 Using FFT. In Silvia Chiappa and Roberto Calandra (eds.), *The 23rd International Conference on
 662 Artificial Intelligence and Statistics, AISTATS 2020, 26-28 August 2020, Online [Palermo, Sicily,
 663 Italy]*, volume 108 of *Proceedings of Machine Learning Research*, pp. 2560–2569. PMLR, 2020.

664 Alex Krizhevsky. Learning Multiple Layers of Features From Tiny Images. Master’s thesis, Uni-
 665 versity of Toronto, 2009.

666 Alex Kulesza, Ananda Theertha Suresh, and Yuyan Wang. Mean Estimation in the Add-Remove
 667 Model of Differential Privacy. In *Forty-first International Conference on Machine Learning,
 668 ICML 2024, Vienna, Austria, July 21-27, 2024*. OpenReview.net, 2024.

669 Saeed Mahloujifar, Luca Melis, and Kamalika Chaudhuri. Auditing $\$f\$$ -Differential Privacy in One
 670 Run. In *Forty-second International Conference on Machine Learning*, 2025.

671 Harsh Mehta, Abhradeep Guha Thakurta, Alexey Kurakin, and Ashok Cutkosky. Towards Large
 672 Scale Transfer Learning for Differentially Private Image Classification. *Trans. Mach. Learn.
 673 Res.*, 2023, 2023.

674 Sebastian Meiser and Esfandiar Mohammadi. Tight on Budget?: Tight Bounds for r-Fold Approx-
 675 imate Differential Privacy. In David Lie, Mohammad Mannan, Michael Backes, and XiaoFeng
 676 Wang (eds.), *Proceedings of the 2018 ACM SIGSAC Conference on Computer and Communi-
 677 cations Security, CCS 2018, Toronto, ON, Canada, October 15-19, 2018*, pp. 247–264. ACM,
 678 2018.

679 Ilya Mironov. Rényi differential privacy. In *30th IEEE Computer Security Foundations Symposium,
 680 CSF 2017, Santa Barbara, CA, USA, August 21-25, 2017*, pp. 263–275. IEEE Computer Society,
 681 2017.

682 Milad Nasr, Shuang Song, Abhradeep Thakurta, Nicolas Papernot, and Nicholas Carlini. Adversary
 683 Instantiation: Lower Bounds for Differentially Private Machine Learning. In *42nd IEEE Sympo-
 684 sium on Security and Privacy, SP 2021, San Francisco, CA, USA, 24-27 May 2021*, pp. 866–882.
 685 IEEE, 2021.

686 Milad Nasr, Jamie Hayes, Thomas Steinke, Borja Balle, Florian Tramèr, Matthew Jagielski,
 687 Nicholas Carlini, and Andreas Terzis. Tight Auditing of Differentially Private Machine Learn-
 688 ing. In Joseph A. Calandrino and Carmela Troncoso (eds.), *32nd USENIX Security Symposium,
 689 USENIX Security 2023, Anaheim, CA, USA, August 9-11, 2023*, pp. 1631–1648. USENIX Asso-
 690 ciation, 2023.

691 Adam Paszke, Sam Gross, Francisco Massa, Adam Lerer, James Bradbury, Gregory Chanan, Trevor
 692 Killeen, Zeming Lin, Natalia Gimelshein, Luca Antiga, Alban Desmaison, Andreas Köpf, Ed-
 693 ward Z. Yang, Zachary DeVito, Martin Raison, Alykhan Tejani, Sasank Chilamkurthy, Benoit
 694 Steiner, Lu Fang, Junjie Bai, and Soumith Chintala. PyTorch: An imperative style, high-
 695 performance deep learning library. In Hanna M. Wallach, Hugo Larochelle, Alina Beygelzimer,
 696 Florence d’Alché-Buc, Emily B. Fox, and Roman Garnett (eds.), *Advances in Neural Infor-
 697 mation Processing Systems 32: Annual Conference on Neural Information Processing Systems 2019,
 698 NeurIPS 2019, December 8-14, 2019, Vancouver, BC, Canada*, pp. 8024–8035, 2019.

702 Natalia Ponomareva, Hussein Hazimeh, Alex Kurakin, Zheng Xu, Carson Denison, H. Brendan
 703 McMahan, Sergei Vassilvitskii, Steve Chien, and Abhradeep Guha Thakurta. How to DP-fy ML:
 704 A Practical Guide to Machine Learning with Differential Privacy. *J. Artif. Intell. Res.*, 77:1113–
 705 1201, 2023.

706 Arun Rajkumar and Shivani Agarwal. A Differentially Private Stochastic Gradient Descent Algo-
 707 rithm for Multiparty Classification. In Neil D. Lawrence and Mark A. Girolami (eds.), *Proceed-
 708 ings of the Fifteenth International Conference on Artificial Intelligence and Statistics, AISTATS
 709 2012, La Palma, Canary Islands, Spain, April 21-23, 2012*, volume 22 of *JMLR Proceedings*, pp.
 710 933–941. JMLR.org, 2012.

711 Nils Reimers and Iryna Gurevych. Sentence-bert: Sentence embeddings using siamese bert-
 712 networks. In Kentaro Inui, Jing Jiang, Vincent Ng, and Xiaojun Wan (eds.), *Proceedings of
 713 the 2019 Conference on Empirical Methods in Natural Language Processing and the 9th Inter-
 714 national Joint Conference on Natural Language Processing, EMNLP-IJCNLP 2019, Hong Kong,
 715 China, November 3-7, 2019*, pp. 3980–3990. Association for Computational Linguistics, 2019.

716 Ahmed Salem, Giovanni Cherubin, David Evans, Boris Köpf, Andrew Paverd, Anshuman Suri,
 717 Shruti Tople, and Santiago Zanella-Béguelin. SoK: Let the Privacy Games Begin! A Unified
 718 Treatment of Data Inference Privacy in Machine Learning. In *44th IEEE Symposium on Security
 719 and Privacy, SP 2023*, pp. 327–345. IEEE, 2023.

720 Reza Shokri, Marco Stronati, Congzheng Song, and Vitaly Shmatikov. Membership Inference At-
 721 tacks Against Machine Learning Models. In *2017 IEEE Symposium on Security and Privacy, SP
 722 2017*, pp. 3–18. IEEE Computer Society, 2017.

723 Richard Socher, Alex Perelygin, Jean Wu, Jason Chuang, Christopher D. Manning, Andrew Ng,
 724 and Christopher Potts. Recursive deep models for semantic compositionality over a sentiment
 725 treebank. In *Proceedings of the 2013 Conference on Empirical Methods in Natural Language
 726 Processing*, pp. 1631–1642, Seattle, Washington, USA, October 2013. Association for Computa-
 727 tional Linguistics.

728 Shuang Song, Kamalika Chaudhuri, and Anand D. Sarwate. Stochastic gradient descent with dif-
 729 fferentially private updates. In *IEEE Global Conference on Signal and Information Processing,
 730 GlobalSIP 2013, Austin, TX, USA, December 3-5, 2013*, pp. 245–248. IEEE, 2013.

731 Thomas Steinke, Milad Nasr, and Matthew Jagielski. Privacy Auditing with One (1) Training Run.
 732 In Alice Oh, Tristan Naumann, Amir Globerson, Kate Saenko, Moritz Hardt, and Sergey Levine
 733 (eds.), *Advances in Neural Information Processing Systems 36: Annual Conference on Neural
 734 Information Processing Systems 2023, NeurIPS 2023, New Orleans, LA, USA, December 10 - 16,
 735 2023*.

736 Marlon Tobaben, Aliaksandra Shysheya, John Bronskill, Andrew Paverd, Shruti Tople, Santi-
 737 ago Zanella Béguelin, Richard E. Turner, and Antti Honkela. On the Efficacy of Differentially
 738 Private Few-shot Image Classification. *Trans. Mach. Learn. Res.*, 2023, 2023.

739 Florian Tramèr and Dan Boneh. Differentially Private Learning Needs Better Features (or Much
 740 More Data). In *9th International Conference on Learning Representations, ICLR 2021, Virtual
 741 Event, Austria, May 3-7, 2021*. OpenReview.net, 2021.

742 Ashkan Yousefpour, Igor Shilov, Alexandre Sablayrolles, Davide Testuggine, Karthik Prasad, Mani
 743 Malek, John Nguyen, Sayan Ghosh, Akash Bharadwaj, Jessica Zhao, Graham Cormode, and Ilya
 744 Mironov. Opacus: User-Friendly Differential Privacy Library in PyTorch. *CoRR*, abs/2109.12298,
 745 2021.

746 Santiago Zanella-Béguelin, Lukas Wutschitz, Shruti Tople, Ahmed Salem, Victor Rühle, Andrew
 747 Paverd, Mohammad Naseri, Boris Köpf, and Daniel Jones. Bayesian Estimation of Differen-
 748 tial Privacy. In *International Conference on Machine Learning, ICML 2023, 23-29 July 2023,
 749 Honolulu, Hawaii, USA*, volume 202 of *Proceedings of Machine Learning Research*, pp. 40624–
 750 40636. PMLR, 2023.

751

756 Puning Zhao, Jiafei Wu, Zhe Liu, Li Shen, Zhikun Zhang, Rongfei Fan, Le Sun, and Qingming
 757 Li. Enhancing learning with label differential privacy by vector approximation. In *The Thirteenth*
 758 *International Conference on Learning Representations, ICLR 2025, Singapore, April 24-28, 2025*.
 759 OpenReview.net, 2025.

761 A APPENDIX

762 A.1 EXPERIMENTAL TRAINING DETAILS

763 Table A1 details the hyperparameters used for training the models for our experiments. We use Opa-
 764 cius (Yousefpour et al., 2021) to facilitate DP training of models with Pytorch (Paszke et al., 2019). In
 765 our experiments, we vary the seed per run, which ensures randomness in mini-batch sampling and,
 766 in the case of models trained from scratch, also ensures random initialization per run.

767 We find that adding a canary to the gradients or datasets does not compromise the utility of the
 768 trained models which we measure in terms of their accuracy on the test dataset. Figure A1 compares
 769 the test accuracies for models poisoned using gradient canaries Algorithm 2 and crafted input canary
 770 Algorithm 3 to models trained with the target record. With $q = 1$, the model “sees” the canary at
 771 each step of training. Despite that, we observe minimal difference in test accuracies averaged across
 772 5 models trained with target record and models trained with either gradient or crafted input canaries.

773 Table A1: Hyperparameters used for the experiments in the main paper. We use these as default
 774 hyperparameters for a given dataset unless otherwise specified.

775 Hyperparameters	776 CIFAR10	777 Purchase100	778 SST-2
779 DP Optimizer	780 DP-SGD	781 DP-Adam	782 DP-SGD
783 Trainable Parameter Count ($ \theta $)	784 768	785 89828	786 384
787 Initialization (θ_0)	788 Fixed	789 Random	790 Fixed
791 Subsampling Rate (q)	792 $(1.0, 0.25, 0.0625)$	793 $(0.25, 0.0625)$	794 (1.0, 0.25)
795 Clipping Bound (C)	796 2.0	797 5.0	798 2.0
799 Training Steps (T)	800 500	801 2500	802 2500
803 Learning Rate η	804 0.001	805 0.0018	806 0.01
Common Settings			
Loss Function			
Subsampling			
Auditing Runs (R)			
δ			
Cross Entropy Loss			
Poisson			
2500			
10^{-5}			

792 A.2 EFFECT OF TRAINING HYPERPARAMETERS ON AUDITING

793 Choice of the clipping bound C only affects audits done using input-space canaries significantly.
 794 This is because gradient-space canaries are crafted using Algorithm 2 which ensures that $\|g_z\|$
 795 and $\|g_{z'}\| = C$ (that is, they have near-saturation gradient norms) throughout the training process.
 796 Thus, the crafted gradient canaries are minimally affected by clipping during training. In contrast,
 797 input-space canaries, specifically, crafted input (Algorithm 3) and adversarial natural canaries (Al-
 798 gorithm 5) show high sensitivity to the choice of C . High C corresponds to higher noise added
 799 during DP which affects the distinguishability between target sample and the canary.

800 In Figure A3, we find that, keeping subsampling rate q fixed ($= 0.0625$), if we vary the number of
 801 training steps T , it affects the auditing with input-space canaries. For a fixed q , a larger T means
 802 that the canary is “seen” more number of times during training. As we keep the total privacy budget
 803 constant, a larger T for a fixed q also implies an increase in the noise accumulated over intermediate
 804 steps. We observe that the audits done with crafted input canary and adversarial natural canaries
 805 suffer with an increase in T , especially at later training steps.

806 Similarly, Figure A4 demonstrates that auditing done with input space canaries is affected by the
 807 choice of learning rate. Thus, we find that canaries crafted/ chosen to mimic samples from training
 808 data are susceptible to the training hyperparameters. In auditing, we assume that the adversary has
 809 access to the hyperparameters. However, in practice, the model trainer might choose to keep these

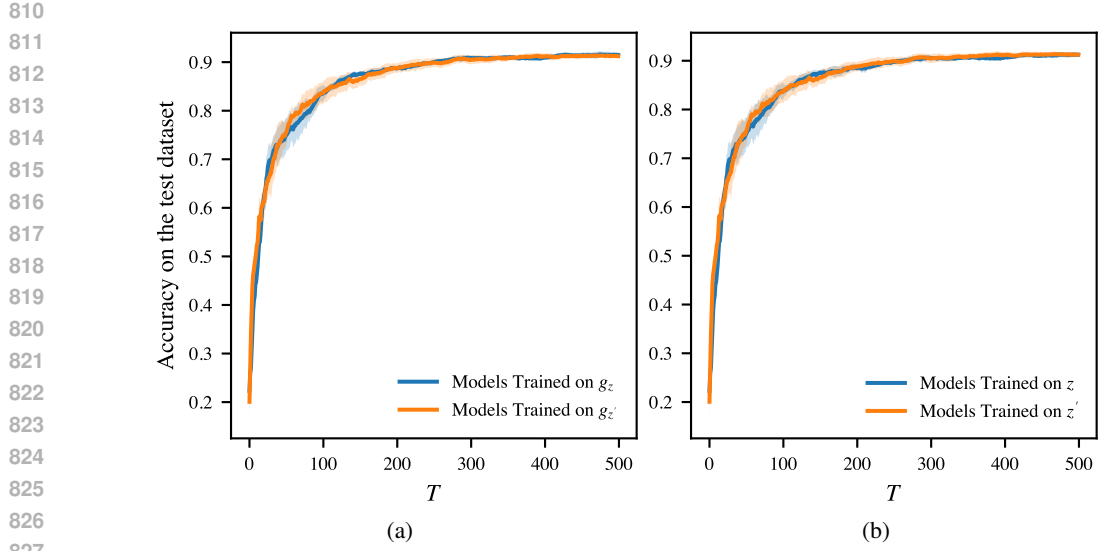


Figure A1: **Auditing with our proposed canaries does not compromise model utility.** The figure depicts test accuracies as observed over the course of training for (a) models trained with gradient canaries (Algorithm 2), and (b) models trained on crafted input canary (Algorithm 3). The model is ViT-B-16 pretrained on ImageNet21K with final layer fine-tuned on CIFAR10. We train the model with $q = 1$ for 500 steps with $\varepsilon = 10$, $\delta = 10^{-5}$ for substitute DP.

hyperparameters confidential. This means that the audits done using such canaries can underestimate privacy leakage suggested by formal DP guarantees.

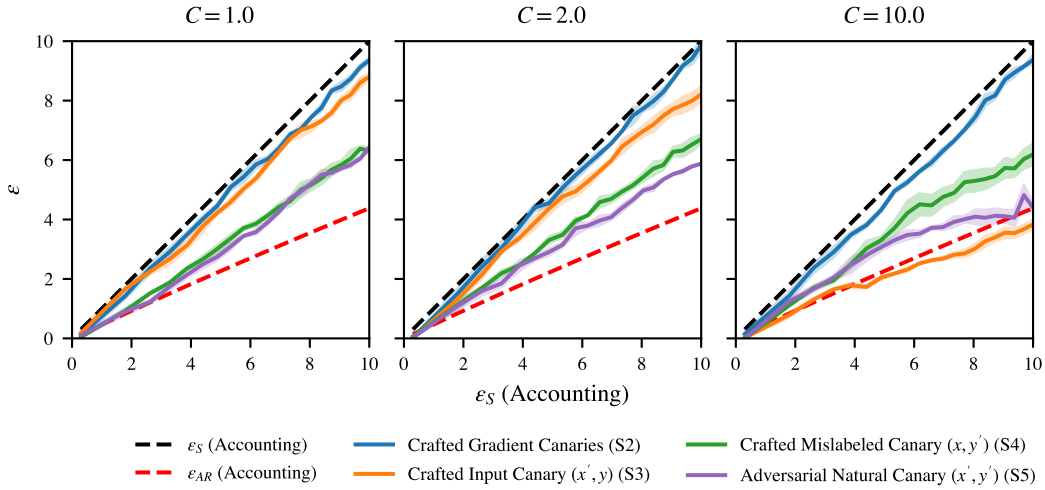


Figure A2: **Effect of clipping bound C on privacy auditing.** For ViT-B-16 models with final layer fine-tuned on CIFAR10 (with $q = 1.0$, $T = 500$), varying C causes crafted input and adversarial natural canary to lose their effectiveness as C increases. Higher C leads to higher per-step noise added during training. This adversely affects the audits using crafted input and adversarial natural canary. Crafted gradient and crafted mislabeled canary show relatively less sensitivity to C . We plot ε for every k th step ($k = 25$) averaged over 3 repeats of the auditing algorithm. For each repeat, we train $R = 2500$ models, $1/2$ trained with z and the remaining with z' . The error bars represent ± 2 standard errors around the mean computed over 3 repeats of auditing algorithm.

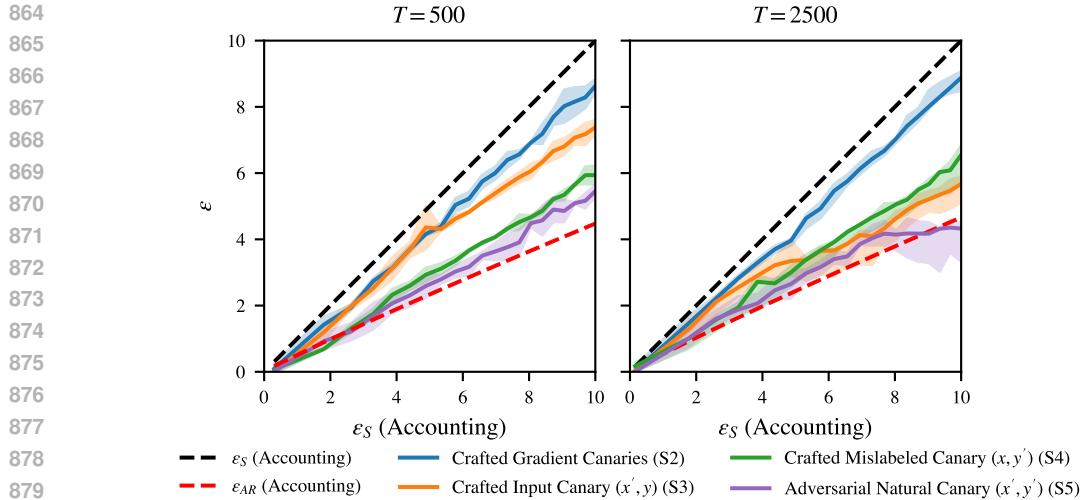


Figure A3: **Effect of training steps T on privacy auditing.** For ViT-B-16 models with final layer fine-tuned on CIFAR10 (with $q = 0.0625, C = 2.0$), varying T with subsampling leads to an increase in the noise accumulated over intermediate steps between successive canary appearances during training. This most significantly affects auditing with crafted input and adversarial natural canary. They yield relatively stronger audits for $T = 500$ but with $T = 2500$, they loose their efficacy for later training steps. As the total privacy budget is fixed for $T = 500$ and $T = 2500$, the degradation in audits for input-space canaries can be attributed to the higher per-step noise associated with larger T . We plot ϵ for every k th step ($k = 25$ for $T = 500$ and $k = 125$ for $T = 2500$) averaged over 3 repeats of the auditing algorithm. For each repeat, we train $R = 2500$ models, $1/2$ trained with z and the remaining with z' . The error bars represent ± 2 standard errors around the mean computed over 3 repeats of auditing algorithm.

A.3 RELATIONSHIP BETWEEN EXPECTED PRIVACY LOSS UNDER SUBSTITUTE DP AND ADD/REMOVE DP

Typically, the privacy loss under substitute DP is expected to be $2\times$ the privacy loss under add/remove DP. However, as shown in Equation (4), this holds true when the δ is also scaled appropriately when moving from add/remove to substitute DP. If we keep the δ constant for add/remove and substitute DP, ϵ_{SR} can be $> 2\epsilon_{AR}$, especially when ϵ is large, that is, when we use a large subsampling rate (q) and low noise (σ), as shown in Figure A5. We also show that this ratio is dependent on changes in q and σ .

A.4 ADDITIONAL RESULTS

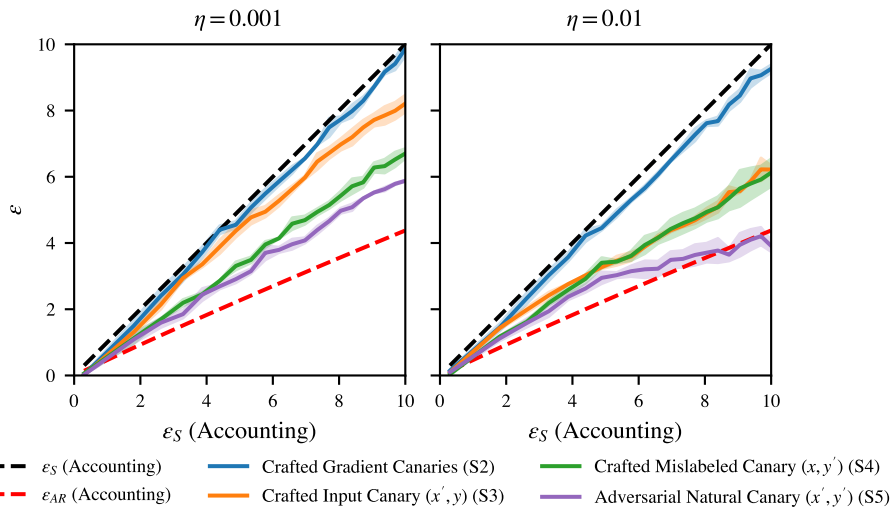


Figure A4: **Effect of learning rate η on privacy auditing.** For ViT-B-16 models with final layer fine-tuned on CIFAR10 (with $q = 1.0, T = 500$), change in η reduces the effectiveness of audits with input-space canaries. We plot ε for every k th step ($k = 25$) averaged over 3 repeats of the auditing algorithm. For each repeat, we train $R = 2500$ models, 1/2 trained with z and the remaining with z' . The error bars represent ± 2 standard errors around the mean computed over 3 repeats of auditing algorithm.

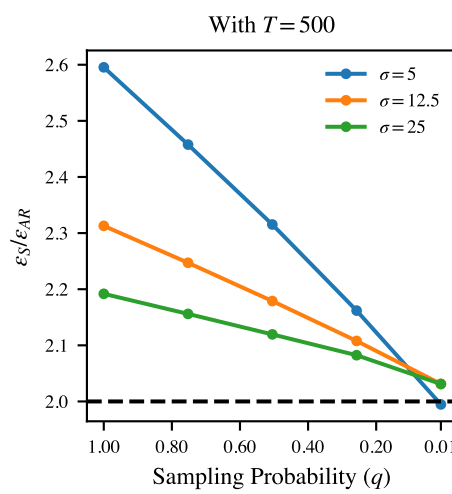


Figure A5: **Relationship between ε_S and ε_{AR} For varying Subsampling Rate (q) and Noise (σ).** The relationship between ε_S and ε_{AR} as defined by Equation (4) is expected to hold when $\delta_S = (1 + e^{\varepsilon_{AR}})\delta_{AR}$. However, for a fixed $\delta_S = \delta_{AR} = 10^{-5}$, we find that ε_S can be $> 2\varepsilon_{AR}$, especially for large q and low σ .

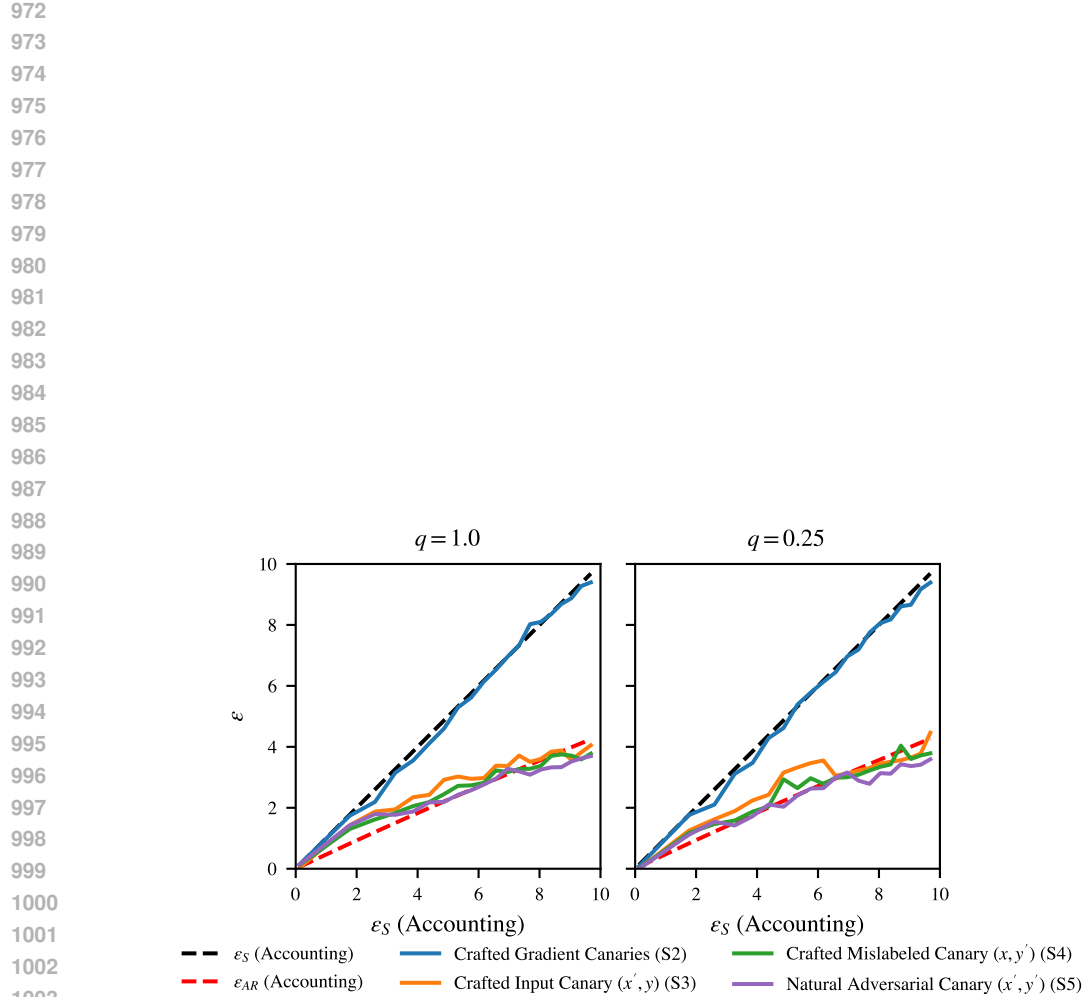


Figure A6: **Auditing Models Trained For Text Classification.** We audit Sentence-BERT models with final linear layer fine-tuned on SST-2 dataset ($C = 2.0$, $T = 2500$). We find that using our canaries, we can extract privacy leakage from these models which may exceed the privacy guaranteed by add/remove DP but is in line with the guarantees of substitute DP. We plot ϵ for every k th step ($k = 125$) of training. For each repeat, we train $R = 2500$ models, $1/2$ trained with z and the remaining with z' .

1010
1011
1012
1013
1014
1015
1016
1017
1018
1019
1020
1021
1022
1023
1024
1025